Biochemical and Biophysical Research Communications 532 (2020) 321–328

Contents lists available at ScienceDirect

Biochemical and Biophysical Research Communications

journal homepage: www.elsevier.com/locate/ybbrc

MicroRNA-31 regulates dental epithelial cell proliferation by targeting *Satb2*

Huizhong Tian [a], Ziwei She [b], Xuejun Gao [a], Weiping Wang [b, **], Hua Tian [a, *]

[a] Department of Cariology and Endodontology, Peking University School and Hospital of Stomatology, National Clinical Research Center for Oral Diseases, National Engineering Laboratory for Digital and Material Technology of Stomatology, Beijing Key Laboratory of Digital Stomatology, PR China
[b] Department of Biochemistry and Biophysics, School of Basic Medical Sciences, Peking University, PR China

ARTICLE INFO

Article history:
Received 14 July 2020
Accepted 29 July 2020
Available online 30 August 2020

Keywords:
Tooth development
Satb2
Cell proliferation
miR-31

ABSTRACT

MicroRNAs (miRNAs) exhibit strong potential clinical application owing to their extensive regulation and flexible delivery properties. MicroRNA-31 (miR-31) is an evolutionarily conserved miRNA expressed during tooth development, and it is highly expressed in mouse incisor epithelium. The specific role of miR-31 in odontogenesis has not been elucidated comprehensively, and the aim of the present study was to investigate its activity. Our results showed that miR-31 suppressed LS8 cell proliferation by inhibiting the cell cycle at the G1/S transition. Mutation of Special AT-rich sequence-binding protein 2 (*SATB2*) gene is responsible for human SATB2-associated syndrome (SAS), which is often accompanied by dental abnormities. Here, it was identified as a direct target of miR-31 in LS8 cells and a promoter of cell proliferation. The expression and distribution of SATB2 in mouse molars and incisors were explored using immunofluorescence, which showed strong signals in the nuclei of incisor epithelial cells and weak signals in the cytoplasm of molar epithelial cells. Moreover, rescue experiments demonstrated that *Satb2* could mitigate the inhibitory effect of miR-31 on cell proliferation by promoting the expression of CDK4. Collectively, our results suggested that miR-31 regulates dental epithelial cell proliferation by targeting *Satb2*, highlighting the biological importance of miR-31 in odontogenesis.

© 2020 Elsevier Inc. All rights reserved.

1. Introduction

Tooth development is a sophisticated physiological process induced by dental epithelial and mesenchymal interactions, which involves numerous signaling pathways, transcription factors, and epigenetic modifications [1]. MicroRNAs (miRNAs) are a family of 19~24 nt non-coding, single-strand RNA molecules, which can post-transcriptionally suppress gene expression by binding to the 3′-UTR of target messenger RNA (mRNA) [2]. MicroRNAs have been shown to regulate the development of various ectodermal-derived tissues such as teeth, hair, skin, and mammary glands [3]. Deletion of *Dicer* in dental epithelium leads to multiple incisors with the absence of enamel and small cuspless molars in mice, suggesting the requirement of miRNAs in tooth patterning, sizing, and shaping [4–6]. A previous study using miRNA microarrays identified eight tissue-and-stage-specific miRNAs involved in tooth formation, including miR-455, miR-689, miR-720, miR-711, miR-141, miR-140, miR-31 and miR-875 [7]. Among them, miR-31 was upregulated during molar morphogenesis and identified as the most differentially expressed miRNA in the labial cervical loop (laCL) compared with the lingual cervical loop and ameloblasts in adult mouse incisors [7,8]. Mouse incisors are characterized by lifelong growth and asymmetrically deposited enamel, which is subjected to the tooth epithelial stem cell niche located in the laCL of the incisor. The expression pattern of miR-31 suggests that it may play a role in the self-renewal and differentiation of dental epithelial stem cells. However, the inherent mechanisms underlying this process are not fully elucidated.

Special AT-rich sequence-binding protein 2 (SATB2) is a highly conserved homeobox protein involved in the determination of craniofacial patterning and osteoblast differentiation [9]. Alterations of *SATB2* in human chromosome 2q32-q33 are responsible for craniofacial dysmorphologies associated with cleft palate, micrognathia, maxillary hypoplasia and dental malformation [10,11]. The phenotypes in *Satb2*$^{-/-}$ mice mimic human deletions in

* Corresponding author. Department of Cariology and Endodontology, School and Hospital of Stomatology, Peking University, 22 Zhongguancun South Avenue, Haidian District, Beijing, 100081, PR China.
** Corresponding author.
E-mail addresses: wwp@bjmu.edu.cn (W. Wang), tianhzh@126.com (H. Tian).

https://doi.org/10.1016/j.bbrc.2020.07.138
0006-291X/© 2020 Elsevier Inc. All rights reserved.

a dosage-dependent manner, presenting as cleft palate, a smaller and shorter tongue, and missing incisors [10–12]. Downregulation of *Pax9*, *Alx4*, and *Msx1*, as well as increased apoptosis, were also observed in the mesenchyme in the craniofacial region of *Satb2*$^{-/-}$ mice [9]. The regulators of *SATB2*/*Satb2* expression and post-transcriptional modifications play critical roles in the etiology of craniofacial defects. The phenotypic correlation of *Satb2* loss with the deletion of miRNA is likely due to miRNAs modulating the proliferation of epithelial progenitor cells in the incisor cervical loops.

It has been widely reported that *Satb2* regulates cell pluripotency, survival and proliferation in organogenesis by targeting the promoters of *Nanog*, *Sox2*, *Klf4*, c-Myc, *Bcl-2* and *XIAP* to transform cells into a progenitor-like phenotype, which indicates that *Satb2* is tightly associated with the cell cycle and proliferation [12–15]. Deng *et al*. reported that the RUNX2-miR-31-SATB2 regulatory loop participates in the osteogenesis, stemness and senescence of bone marrow-derived mesenchymal stem cells [16,17]. However, the relevance between miR-31 and *Satb2* in dental epithelial cell proliferation and self-renewal has not been reported.

In this study, the relationship between miR-31 and *Satb2* and their effects on the proliferation of LS8 cells were investigated. Furthermore, the expression pattern of SATB2 during mouse tooth development was explored. This study will contribute to the further understanding of miR-31 in odontogenesis.

2. Methods and materials

2.1. Cell transfection

Mouse ameloblast-like cells named LS8 cells were kindly provided by Dr. Malcolm Snead (USC, Los Angeles, CA, USA) and cultured in high-glucose Dulbecco's modified Eagle's medium (DMEM, Gibco, USA) with 10% fetal bovine serum. For cell transfection, reagents and plasmids including mmu-miR-31 mimics, mimics NC (negative control), mmu-miR-31 inhibitor, inhibitor NC (RioBoBio, China), si*Satb2*, siRNA NC (RioBoBio, China), *Satb2* expression plasmid *p-Satb2* (Origene Bio, China) and Vector *p*-CMV6 were transiently transfected into LS8 cells. The transfection was conducted in Opti-MEM (Invitrogen, USA) with optimal volume of Lipo2000. The sequences of si01 are: sense UAUUUGCUGCCUGACAAGCtt; antisense GCUUGUCAGGCAGCAAAUAtt. The sequences of si02 are: sense UUAACUGCUCUGGGAAUGGtt; antisense CCAUUCCCAGAGCAGUUAAtt. The sequences of siRNA NC are: sense UUCUCCGAACGUGUCACGUtt; antisense ACGUGACACGUUCGGAGAAtt.

2.2. Quantitative real-time PCR

Total RNA was isolated using TRIzols reagent (Invitrogen, USA). 2 μg of RNA was reverse-transcribed into cDNA by the Superscript first-strand synthesis system (Takara, Japan) according to the protocol. qPCR reactions were performed in a 10-μL reaction mixture using an ABI 7300 real-time PCR system (Applied Biosystems, USA). The mRNA expressions were standardized by β-actin and calculated using the $2^{-\Delta\Delta Ct}$ method. Primers for amplification were shown in Table 1.

2.3. Quantitative analysis of miRNA expression

RNA was reverse-transcribed into miR-cDNA using miRcute Plus miRNA First-Strand cDNA Synthesis Kit. The real-time PCR was performed with the miRcute Plus miRNA qPCR Detection Kit. The expression was standardized by murine U6. All agent kits and primers were purchased from (TIANGEN, China).

Table 1
The primers for PCR (5′–3′).

Name	Forward (5′-3′)	Reverse (5′-3′)
Satb2	CCGTGGGAHHTTTGATGATT	GTGCTCTTCTCGGTTGTCGT
Cyclin D1	TCAAGTGTGAACCCGGACTGC	CCTTGGGGTCGACGTTCTG
Cyclin A2	TCTCACTACATAGCTGACTTGGAC	TCTCACTACATAGCTGACTTGGAC
Cyclin E1	TATGGTGTCCTCGCTGCTTC	GTCGCACCACTGATAACCTGA
Cyclin B1	TCTCGAATCGGGGAACCTCT	GCCATACTGACCTTGGCCTT
β-actin	GCCTTCCTTCTTGGGTATG	ACCACCAGACAGCACTGTG

2.4. Western blot assay

Proteins were extracted with RIPA containing protease inhibitor and determined by BCA Protein Assay Kit (Pierce, USA). Each sample was subjected to SDS-PAGE and transferred to a PVDF membrane (Millipore, USA). After blocked, The membrane was incubated with the primary antibodies, *anti*-SATB2 (Santa Cruz, sc-81376), *anti*-Cyclin D1 (Abclonal, NO: 2706), *anti*-E2F1 (Huabio, ET1701-73) and *anti*-CDK4 (Abclonal, NO: A0366) overnight and with the HRP-conjugated secondary antibodies (Rockland, USA) for 1 h. Protein bands were exposed and then visualized by Odyssey infrared imaging system (Odyssey LI-COR Biosciences, USA).

2.5. CCK8 and EdU-incorporated assay

The proliferation of LS8 cells was assessed by the cell counting kit-8 (CCK8) (Dojindo, Japan) and Cell-Light^{TM}EdU Apollo®567 In Vitro Kit (RioBoBio, China) respectively, according to the manufacturers' instructions. 2×10^3 cells per well with 100 μl complete medium were plated onto 96-well plates and cultured overnight at 37 °C. For CCK8 assay, 10% CCK8 solution in culture medium was replaced after 24, 48 and 72 h from transfection respectively. Plates were incubated at 37 °C for 1.5 h. The optical density (OD) was measured by a microplate reader (iMark, USA). For EdU-incorporated assay, the cells were cultured after 48 h from transfection, then replaced with 50 μM EdU culture medium and cells were cultured for additional 2.5 h at 37 °C. Nuclei were stained with Hoechst 33342. The EdU-positive cells and total cells were counted and the ratio were calculated and statistically analyzed.

2.6. Flow cell cycle analysis

Cells were cultured and transfected in 6-well plate, washed and fixed in ice-cold 70% ethanol. 100 mg/mL propidium iodide solution (containing Rnase inhibitor) was incubated in dark. DNA content was subsequently subjected to cell cycle analysis. The numbers of cells in the G1, S, and G2 phases were analyzed.

2.7. Luciferase reporter assay

The predicted binding site of mmu-miR-31 in the *Satb2* mRNA 3′-UTR was cloned downstream of the rinia luciferase gene and upstream of the firefly luciferase gene in the pmiR-RB-REPORT™ Vector (RioBoBio, China). LS8 cells were seeded in 24-well plates and co-transfected with *Satb2*-3′-UTR-WT or *Satb2*-3′-UTR-MUT, with miR-31 mimics or NC using Lipo 2000. Cells were harvested after 24 h and assayed for Renilla and Firefly luciferase activity using the Dual-Lucy Assay Kit (promega, China).

2.8. Preparation of tissue sections and immunofluorescence

All experiments and protocols were permitted by Animal Care and Use Committee of Peking University (Permit number: LA2019025). Pregnant mice from different developmental stages (E13.5, E14.5, E16.5, n ≥ 6) and neonatal mice (PN0, n ≥ 6) were

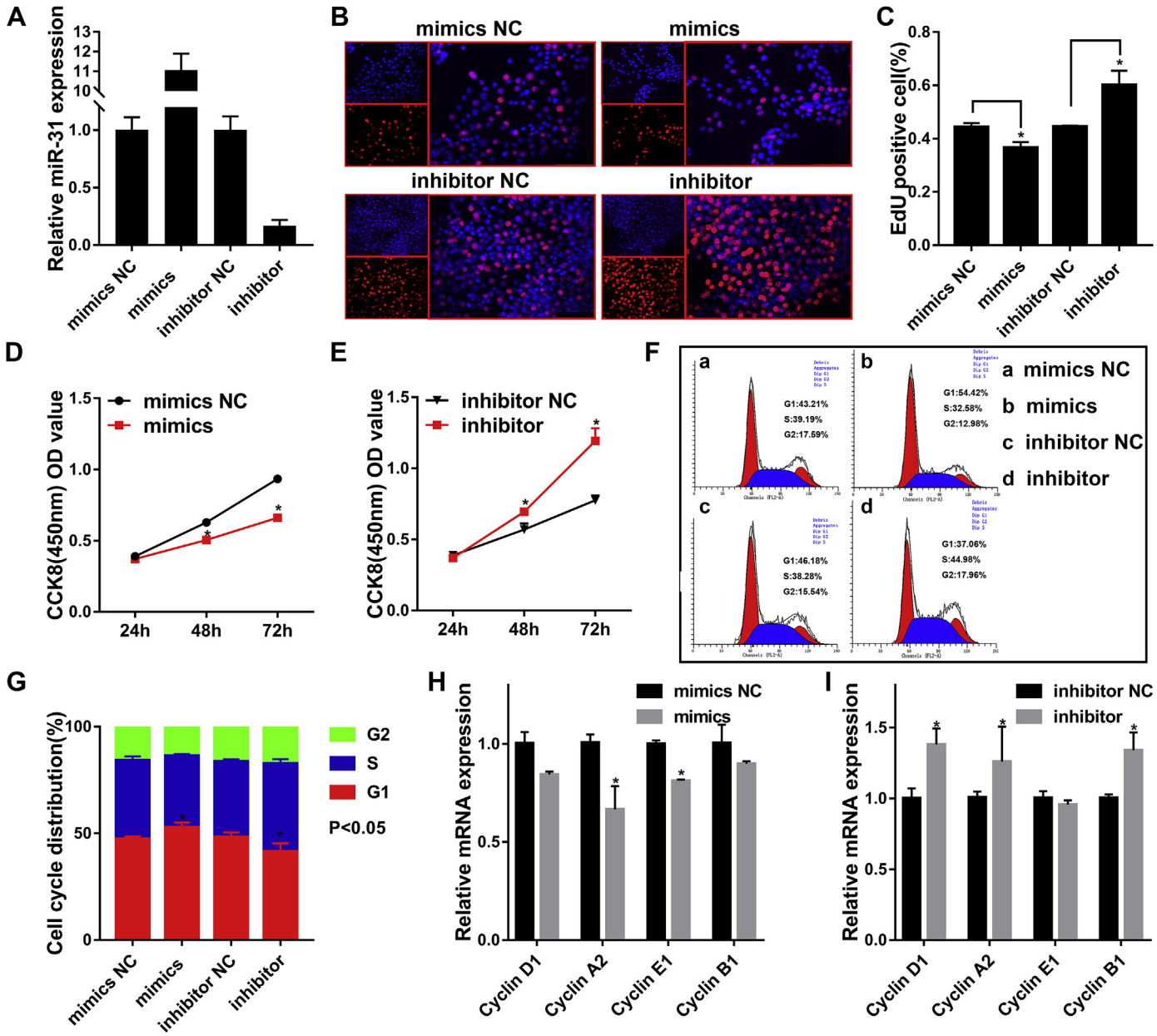

Fig. 1. miR-31 inhibits dental epithelial cell proliferation by causing G1/S phases arrest. qPCR assay identified the efficiency of miR-31 mimics and inhibitor in LS8 cells (A). The cell proliferation ability was assessed by EdU-incorporated assay after transfection (B) and its quantitative analysis (C). OD value in LS8 cells after transfected with miR-31 mimics (D) and inhibitor (E). Cell cycle distribution of LS8 transfected cells was analyzed by Flow cytometry (F) and its quantitative analysis (G). The mRNA expression of genes associated with G1/S transition were regulated by miR-31 mimics (H) and inhibitor (I). Data represent means ± SD. *$p < 0.05$. NC, negative control.

sacrificed, mandibles of mice were separated and collected. All samples were fixed in 4% paraformaldehyde, dehydrated, embedded in paraffin. For immunofluorescence, the samples were deparaffinized, rehydrated and antigen retrieval. The sections were blocked and further incubated with primary antibodies, *anti*-SATB2 (SantaCruz, sc-81376, 1:100) and *anti*-CDK4 (Abclonal, NO:A0366, 1:100) overnight at 4 °C, with PBS as negative control. Goat anti-rabbit fluorescent secondary antibody (1:200) and Goat anti-mouse fluorescent secondary antibody (1:200) were then applied and DAPI was used for counterstaining, finally the slices were visualized under laser scanning confocal microscope.

2.9. Statistical analysis

All data were representatives of each assay repeated independently no less than three times. Data were compared and analyzed using the Student's t-test and one-way Anova with GraphPrism7 software (USA) and presented as mean ± SD. A significant difference was considered when *$p < 0.05$.

3. Results

3.1. miR-31 regulates proliferation of dental epithelial cells by mediating cell cycle procession

To explore the effect of miR-31 on the proliferation of dental epithelial cells, mimics and inhibitor were transfected into LS8 cells to alter the expression of miR-31. qPCR was performed to confirm their efficiency (Fig. 1A), and cell proliferation was analyzed after transfection. EdU-incorporation assay demonstrated that the

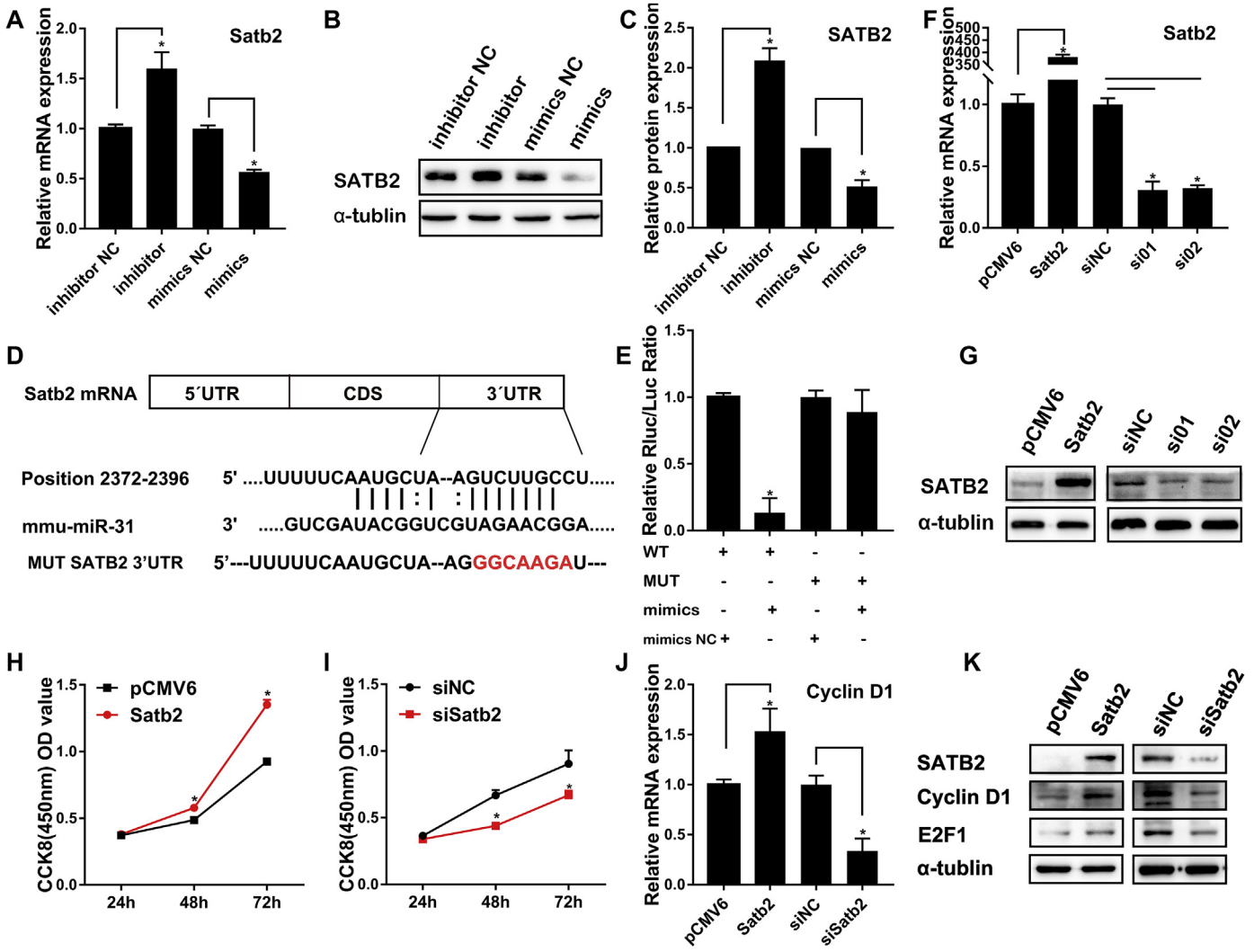

Fig. 2. *Satb2* is a direct target of miR-31 in LS8 cells and promotes cell proliferation. The expression of *Satb2* was regulated by miR-31 mimics and inhibitor on mRNA (A) and protein (B, C) levels. Position 2372–2394 of the 3′-UTR of *Satb2* and its mutation sequence were designed (D). The luciferase activity of *Satb2*-3′UTR-WT or *Satb2*-3′UTR-MUT was assayed with miR-31 mimics or mimic NC co-transfection (E). qPCR and Western blot assay verified the efficiency of si*Satb2* and *p-Satb2* plasmid on mRNA (F) and protein (G) level. OD value in LS8 cells transfected with murine *Satb2* expression plasmid (H) and si*Satb2* (I). The mRNA expression of *Cyclin D1* was determined by transfection with *Satb2* expression plasmid or si*Satb2* (J). The protein expression of Cyclin D1 and E2F1 were determined by transfection with *Satb2* expression plasmid or si*Satb2* (K). Data represent means ± SD. *$p < 0.05$. NC, negative control.

proliferation was increased 1.36 fold in the inhibitor group, whereas in the mimics group, cell proliferation was reduced by 19% compared to the negative control (NC) group, suggesting that miR-31 negatively regulated cell proliferation (Fig. 1B and C). Consistently, CCK8 assay also confirmed the negative effect of miR-31 on cell proliferation (Fig. 1D and E). Furthermore, flow cytometry and qPCR assay were performed to clarify the regulatory effects of miR-31 on LS8 cell proliferation. Elevation of miR-31 arrested the cell cycle in G1 phase (from 47.31% ± 0.99%–52.76% ± 1.89%), whereas suppression of miR-31 facilitated the G1/S transition in LS8 cells, exhibiting a decrease in the proportion of cells in G_1 phase (from 48.18 ± 1.82% to 41.44 ± 1.62%) and an increase in the proportion of cells in S phases (from 35.50 ± 0.82% to 41.27 ± 1.65%) (Fig. 1F and G). Accordingly, associated genes which switch on G1/S transition like *Cyclin D1*, *Cyclin E1*, *Cyclin A2* were slightly repressed in response to miR-31 elevation and vice versa (Fig. 1H and I). Together, these findings indicated that miR-31 suppresses dental epithelial cell proliferation by blocking G1/S transition.

3.2. *Satb2* is regulated by miR-31 in LS8 cells and promotes cell proliferation

It has been reported that *Satb2* is a target gene of miR-31 [16,17]. To verify the relevance of miR-31 and *Satb2* in dental epithelial cells, Western blot and qPCR assay were carried out after transfecting miR-31 inhibitor and mimics in LS8 cells. Expression of *Satb2* was oppressed by miR-31 mimics, and augmented by the inhibitor at both mRNA and protein levels (Fig. 2A, B, C). To ascertain their relationship, a dual-luciferase reporter assay was conducted. The binding site of miR-31 on *Satb2* mRNA is located on the 3′-UTR, and both wild and mutated sequences are shown in Fig. 2D. Relative luciferase activity of *Satb2*-3′-UTR-WT decreased by 75% in response to miR-31 elevation compared to the NC group. There was no significant reduction in luciferase activity in the *Satb2*-3′-UTR-MUT group (Fig. 2E). The results suggested that miR-31 could directly target the 3′-UTR of *Satb2* to inhibit its expression.

After confirming the direct relationship between miR-31 and *Satb2* in LS8 cells, we next investigated the role of *Satb2* on cell

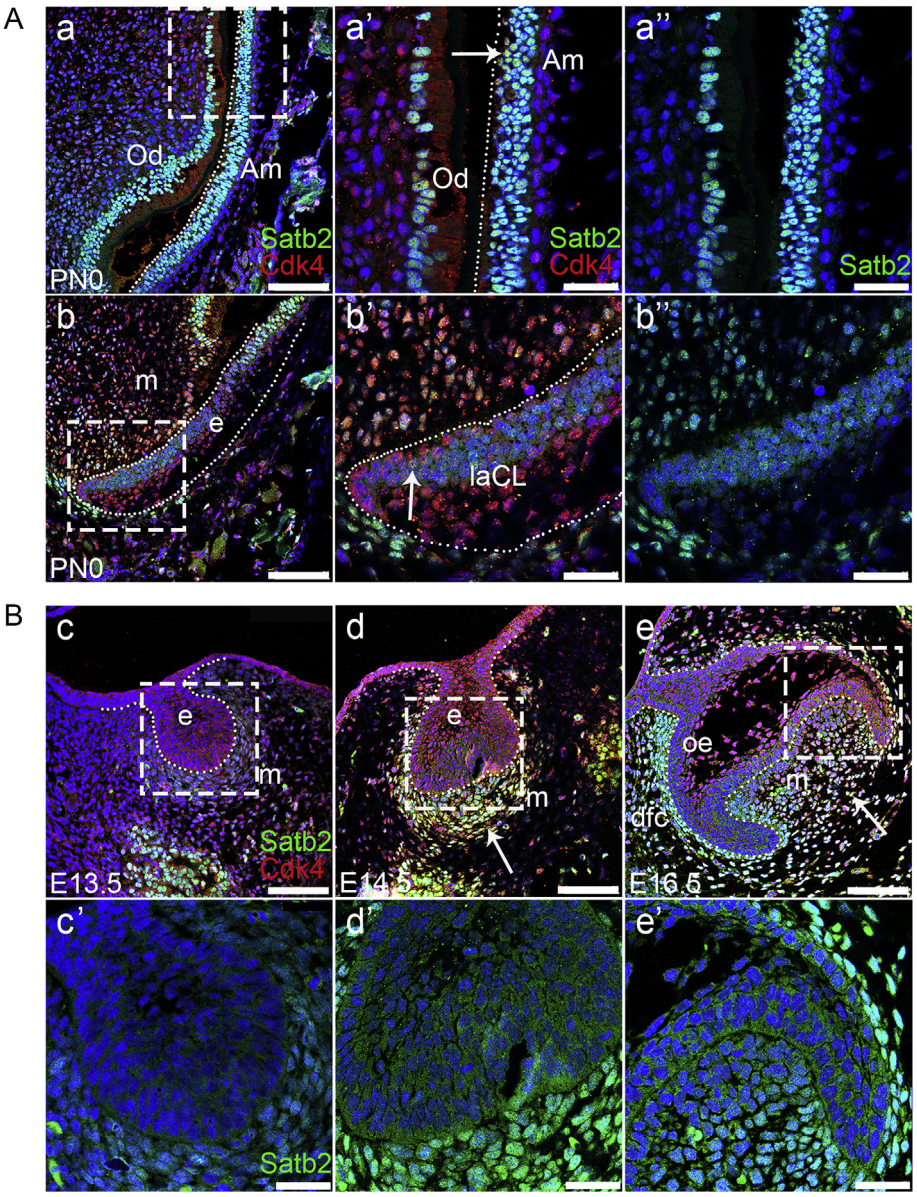

Fig. 3. The expression pattern of SATB2 in mouse incisor and molar. The expression pattern of SATB2 and CDK4 in incisor, immunostaining of SATB2 (green), CDK4 (red) and DAPI (blue) (A). The expression pattern of SATB2 and CDK4 in developing lower M1 germs of mouse embryo (E13.5, E14.5, and E16.5) (B). m, mesenchyme. e, epithelium. Od, odontoblasts. Am, Ameloblasts. laCL, labial cervical loop. oe, outer enamel epithelium. dfc, dental follicle cells. Scar bar=75 μm. Dashed Box shows the Region Zoom. "'" & """ represents image at higher magnification; Scar bar=25 μm."→"arrows indicate the co-localization. n ≥ 6. (For interpretation of the references to colour in this figure legend, the reader is referred to the Web version of this article.)

proliferation. The cells were transfected with either a *Satb2* murine expression plasmid or *Satb2* siRNA. qPCR and Western blot analysis validated the aforementioned efficiency (Fig. 2F and G). CCK8 assay showed that the upregulation of *Satb2* promoted LS8 cell proliferation and the downregulation had the opposite effect (Fig. 2H and I). The Expression of cyclin D1 and E2F1, which are critical for cell cycle G1/S transition, increased and decreased in a linear manner with the SATB2 expression (Fig. 2J and K), further supporting the results of the CCK8 assay. Together, these data demonstrated that *Satb2*, a target of miR-31, could promote LS8 cell proliferation by regulating *cyclin D1* and *E2F1*.

3.3. Expression patterns of SATB2 in mouse incisors and molars

To identify the spatial-temporal expression pattern of SATB2 in tooth development, immunofluorescence was performed in developing mouse incisor and molars. SATB2 was highly expressed in the nuclei of differentiated ameloblasts and adjacent mesenchymal-derived odontoblasts in the PN0 incisor (Fig. 3A–a,a',a") and weakly detected in the laCL (Fig. 3A–b,b',b"). In molars, the signals were restricted to the condensing dental mesenchyme at E13.5 and E14.5, which represent the bud and cap stages of the tooth germ (Fig. 3B–c,c', d,d'). At E16.5, SATB2 was detected in both the dental papilla and dental follicle cells, with weaker signals in the cytoplasm of dental epithelial cells compared to the mesenchyme (Fig. 3B–e,e'). Cyclin-dependent kinase 4 (CDK4), a protein that interacts with Cyclin-D1 to participate cell proliferation by promoting G1/S transition [18], could be detected both in the epithelium and mesenchyme in developing molars and incisors. CDK4 co-localized with SATB2 in incisor epithelial cells

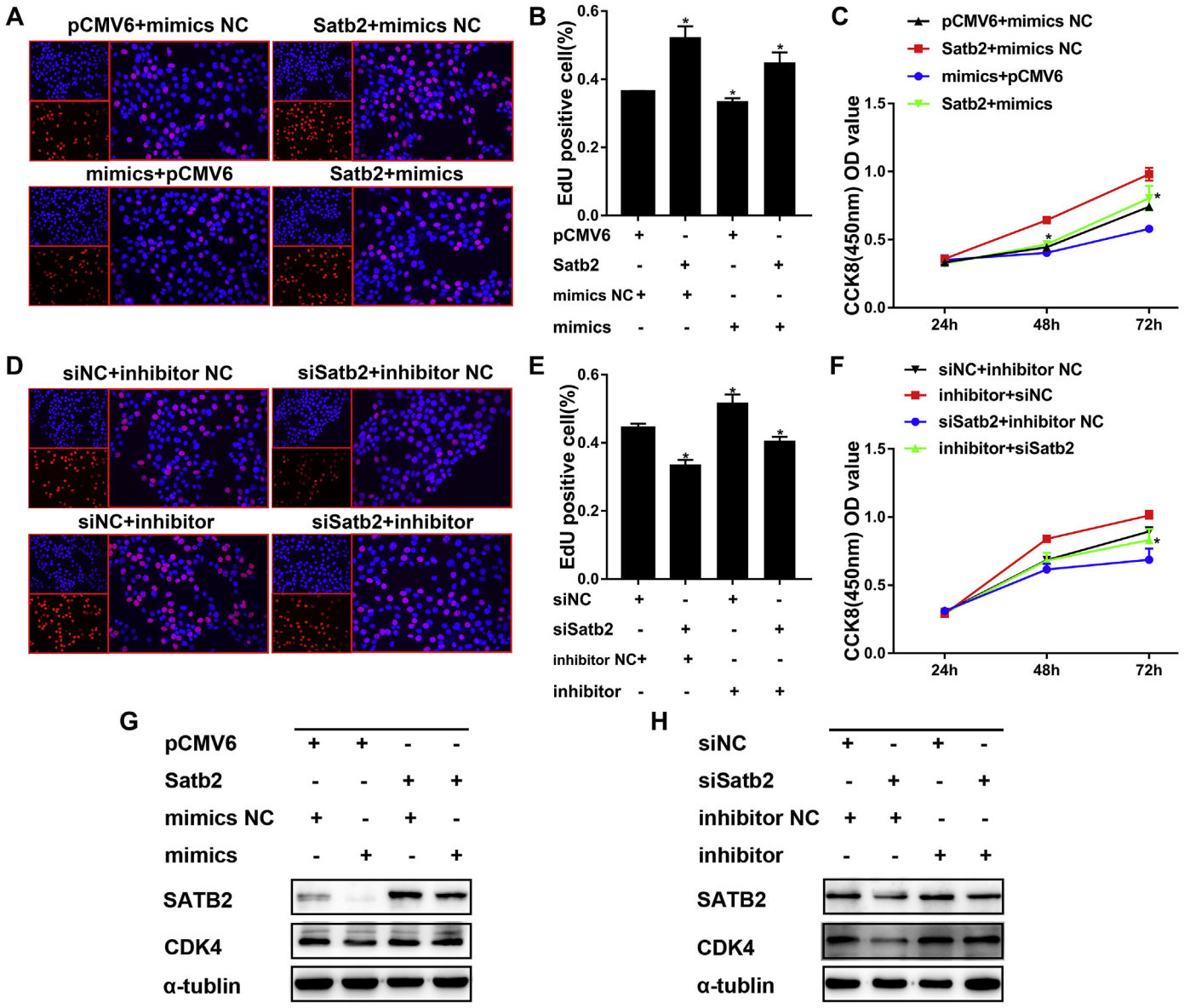

Fig. 4. *Satb2* could partially rescue the effects on proliferation caused by miR-31. The cell proliferation ability was assessed by EdU staining and CCK8 assay after cells transfected with mimics + p-CMV6, mimics NC + p-CMV6, *Satb2*+mimics NC, mimics + *Satb2* (A, B, C) and inhibitor + siRNA NC, inhibitor NC + siRNA NC, si*Satb2*+inhibitor NC, si*Satb2*+inhibitor (D, E, F). (B, F) their quantitative analysis of the EdU staining in (A, D). The protein expression of SATB2 and CDK4 in co-transfection cells (G, H). Data represent means ± SD. *$p < 0.05$. NC, negative control.

(Fig. 3A) and mesenchymal cells in molars (Fig. 3B).

3.4. Satb2 could partially rescue the effects on cell proliferation caused by miR-31

To further investigate whether miR-31 restricted dental epithelial cell proliferation through *Satb2*, the miR-31 mimics or inhibitor were co-transfected with *Satb2* murine expression plasmid or *Satb2* siRNA into LS8 cells. CCK8 and EdU proliferation assays were employed to examine the effect of miR-31/*Satb2* interaction on the proliferation of LS8 cells. The results demonstrated that the reduction in the proliferation of LS8 cells caused by miR-31 mimics was reversed by the overexpression of *Satb2* (Fig. 4A, B, C). Conversely, the increase in proliferation by miR-31 inhibitors was reversed by silencing *Satb2* via its siRNA (Fig. 4D, E, F). Western blot analysis was performed to validate this finding, and the results of this analysis suggested that the rise or fall of miR-31 expression levels altered the protein expression of SATB2 and CDK4 respectively. SATB2 expression could correspondingly reverse this alteration (Fig. 4G and H). Overall, these data indicated that *Satb2* could rescue the effect of miR-31 on LS8 cell proliferation, possibly through CDK4.

4. Discussion

Dental epithelial stem cells reside at the proximal end of the mouse incisor, called the cervical loop, which constantly give rise to ameloblasts, contributing to the sustained deposition of dental enamel. Therefore, mouse incisor is regarded as an ideal model to explore the reciprocal interaction between epithelium and mesenchyme, thus provide biological clues in tooth development and tissue regeneration. To address the posttranscriptional role of

miR-31 on dental epithelial cell proliferation, we analyzed the relevance of miR-31 and *Satb2* and their role in dental epithelial cell proliferation by histomorphology and cellular functional assays. Our study suggested that miR-31 inhibited dental epithelial cell proliferation by targeting 3′-UTR of *Satb2*.

Former studies have demonstrated a strong expression of miR-31 in the incisor epithelium, especially in the laCL [6–8]. Besides, miR-31 has been detected in hair follicle cells, contributing to the equilibrium of hair follicle growth by inhibiting *Dlx3*, *Fgf10*, and related keratin genes [19]. The similarity between the hair follicle stem cell niche and the laCL renders it plausible that miR-31 regulates the homeostasis of self-renewal by fine-tuning cell proliferation in mouse incisors. In our *in vitro* study, we revealed the suppressive role of miR-31 on cell proliferation by altering its endogenous expression. This anti-proliferative effect was exerted through the regulation of cell cycle G1/S transition.

Homeobox genes play significant roles in craniofacial development and tooth patterning [9,20,21]. Dental manifestations in SAS patients include root dysplasia, crown morphological abnormity, teeth crowding and taurodontism [10,11]. In osteogenesis, miRNAs mediate the SATB2/RUNX2 pathway to regulate osteoblast proliferation and differentiation [22]. Bioinformatic analysis indicated that miR-31 potentially targets homeobox genes such as *Satb2*, *Tbx1*, and *Foxj* in odontogenesis. *Satb2* was previously reported to promote cell cycle procession and DNA replication in pre-osteoblasts and maintain Nanog levels to restrain senescence in bone mesenchymal stem cells [12,13]. Furthermore, it could directly activate Wnt signaling and upregulate *Cyclin D1* and *c-Myc* to expedite cell proliferation [23]. Here, *Satb2* stimulated LS8 cell proliferation by positively regulating *Cyclin D1* and E2F1. *Satb2* and miR-31 conversely affected proliferation in LS8 cells, suggesting the potential regulation of miR-31 via *Satb2* on cell proliferation. To verify this, their target-relationship in LS8 cells was investigated, and it was found that miR-31 could directly bind to the site 2372–2394 in the 3′-UTR of *Satb2* mRNA to inhibit its expression at both the mRNA and protein level.

Moreover, SATB2 was found to be expressed in the labial dental epithelium in neonatal mouse incisors, with stronger signals in differentiated ameloblasts compared to those in undifferentiated cells in the cervical loop. This provided indirect evidence that miR-31 potentially regulates *Satb2* in the proliferation of dental epithelial cells. A cell proliferation rescue experiment was executed, and the expression of SATB2 and CDK4 was analyzed. The results showed that the impact of miR-31 on cell proliferation is reliant upon *Satb2*.

Interestingly, in contrast to the incisor, SATB2 was strongly expressed in the molar mesenchymal cells, compared to weak signals in the cytoplasm of epithelial cells. In the early stage of tooth development, the underlying mesenchyme is of great significance in inducing the primary enamel knot formation. The different expression pattern between molars and incisors is consistent with the phenotype reported in *Satb2*$^{-/-}$ mice, which exhibited missing incisors and slightly affected molars [9], indicating distinct roles of *Satb2* in tooth patterning. Additionally, intense signals were also detected in dental follicle cells surrounding the external enamel epithelium at E16.5, which is supported by Deng *et al.* [24]. It has been reported that *Satb2* is weakly expressed in human adult epithelial cells and overexpression in normal epithelial cells would result in a progenitor-like phenotype [14,15]. The strong signals in the nuclei of incisor epithelial cells and undetectable signal in molars indicated that *Satb2* may play a crucial role in the continuous growth of incisors and contribute to the different fates of mouse molars and incisors. The specific mechanism of action requires further study.

In general, our studies suggested a suppressive role of miR-31 on dental epithelial cell proliferation through targeting 3′-UTR of *Satb2* mRNA. Recently, microRNA has attracted tremendous attention as target-delivery drug molecules in clinical treatment and regeneration medicine [25]. Exploring the regulation of miRNAs in odontogenesis would envision a promising future in tooth restoration and regeneration.

Author contributions

H. T performed experiments and analyzed the data. ZW.S assisted in performance and analysis. H.T, X. G managed the project. H.T, H.T, WP·W designed and managed the project and wrote the paper. All authors discussed the results and commented on the manuscript.

Funding

This study is supported by the National Natural Science Foundation of China to Hua Tian (81300839) and Xuejun Gao (81570943).

Declaration of competing interest

Authors declare no conflict of interest.

Acknowledgments

We thank Prof. Xiaoyan Wang and Prof. Xiaowei Zhang from Peking University for their innovative recommendations to this research.

References

[1] A. Balic, I. Thesleff, Tissue interactions regulating tooth development and renewal, Curr. Top. Dev. Biol. 115 (2015) 157–186.
[2] J. O'Brien, H. Hayder, Y. Zayed, et al., Overview of MicroRNA biogenesis, mechanisms of actions, and circulation, Front. Endocrinol. 9 (2018) 402.
[3] N.A. Stepicheva, J.L. Song, Function and regulation of microRNA-31 in development and disease, Mol. Reprod. Dev. 83 (8) (2016) 654–674.
[4] H. Cao, J. Wang, X. Li, et al., MicroRNAs play a critical role in tooth development, J. Dent. Res. 89 (8) (2010) 779–784.
[5] S. Oommen, Y. Otsuka-Tanaka, N. Imam, et al., Distinct roles of microRNAs in epithelium and mesenchyme during tooth development, Dev. Dynam. 241 (9) (2012) 1465–1472.
[6] F. Michon, M. Tummers, M. Kyyronen, et al., Tooth morphogenesis and ameloblast differentiation are regulated by microRNAs, Dev. Biol. 340 (2) (2010) 355–368.
[7] A.M. Jevnaker, H. Osmundsen, MicroRNA expression profiling of the developing murine molar tooth germ and the developing murine submandibular salivary gland, Arch. Oral Biol. 53 (7) (2008) 629–645.
[8] A.H. Jheon, C.Y. Li, T. Wen, et al., Expression of microRNAs in the stem cell niche of the adult mouse incisor, PLoS One 6 (9) (2011), e24536.
[9] G. Dobreva, M. Chahrour, M. Dautzenberg, et al., SATB2 is a multifunctional determinant of craniofacial patterning and osteoblast differentiation, Cell 125 (5) (2006) 971–986.
[10] J. Scott, C. Adams, S. Beetstra, et al., SATB2-associated syndrome (SAS) and associated dental findings, Spec. Care Dent. 39 (2) (2019) 220–224, https://doi.org/10.1111/scd.12340.
[11] J. Scott, C. Adams, K. Simmons, et al., Dental radiographic findings in 18 individuals with SATB2-associated syndrome, Clin. Oral Invest. 22 (8) (2018) 2947–2951.
[12] P. Zhou, G. Wu, P. Zhang, et al., SATB2-Nanog axis links age-related intrinsic changes of mesenchymal stem cells from craniofacial bone, Aging 8 (9) (2016) 2006–2011.
[13] T. Dowrey, E.E. Schwager, J. Duong, et al., Satb2 regulates proliferation and nuclear integrity of pre-osteoblasts, Bone 127 (2019) 488–498.
[14] Y. Li, Y. Liu, Y. Hu, et al., Special AT-rich sequence-binding protein 2 acts as a negative regulator of stemness in colorectal cancer cells, World J. Gastroenterol. 22 (38) (2016) 8528–8539.
[15] W. Yu, Y. Ma, A.C. Ochoa, et al., Cellular transformation of human mammary epithelial cells by SATB2, Stem Cell Res. 19 (2017) 139–147.
[16] Y. Deng, S. Wu, H. Zhou, et al., Effects of a miR-31, Runx2, and Satb2 regulatory loop on the osteogenic differentiation of bone mesenchymal stem cells, Stem Cell. Dev. 22 (16) (2013) 2278–2286.
[17] L. Xu, Y. Fu, W. Zhu, et al., microRNA-31 inhibition partially ameliorates the

deficiency of bone marrow stromal cells from cleidocranial dysplasia, J. Cell. Biochem. 120 (6) (2019) 9472–9486.
[18] H. Matsushime, M.E. Ewen, D.K. Strom, et al., Identification and properties of an atypical catalytic subunit (p34PSK-J3/cdk4) for mammalian D type G1 cyclins, Cell 71 (2) (1992) 323–334.
[19] A.N. Mardaryev, M.I. Ahmed, N.V. Vlahov, et al., MicroRNA-31 controls hair cycle-associated changes in gene expression programs of the skin and hair follicle, Faseb. J. 24 (10) (2010) 3869–3881.
[20] S. Suryadeva, M.B. Khan, Role of homeobox genes in tooth morphogenesis: a review, J. Clin. Diagn. Res. 9 (2) (2015) ZE09–12.
[21] Z. Zhang, H. Tian, P. Lv, et al., Transcriptional factor DLX3 promotes the gene expression of enamel matrix proteins during amelogenesis, PloS One 10 (3) (2015), e0121288.
[22] M.Q. Hassan, J.A.R. Gordon, M.M. Beloti, et al., A network connecting Runx2, SATB2, and the miR-23ā27ā24-2 cluster regulates the osteoblast differentiation program, Proc. Natl. Acad. Sci. U.S.A 107 (46) (2010) 19879–19884.
[23] W. Yu, Y. Ma, S. Shankar, et al., SATB2/beta-catenin/TCF-LEF pathway induces cellular transformation by generating cancer stem cells in colorectal cancer, Sci. Rep. 7 (1) (2017) 10939.
[24] J. Ge, S. Guo, Y. Fu, et al., Dental follicle cells participate in tooth eruption via the RUNX2-MiR-31-SATB2 loop, J. Dent. Res. 94 (7) (2015) 936–944.
[25] R. Rupaimoole, F.J. Slack, MicroRNA therapeutics: towards a new era for the management of cancer and other diseases, Nat. Rev. Drug Discov. 16 (3) (2017) 203–222.